

$t - J$ model one-electron renormalizations: high energy features in photoemission experiments of high- T_c cuprates.

Andrés Greco

Facultad de Ciencias Exactas, Ingeniería y Agrimensura and Instituto de Física Rosario (UNR-CONICET). Av. Pellegrini 250-2000 Rosario-Argentina.

(Dated: April 19, 2018)

Recent angle-resolved photoemission experiments in hole doped cuprates reported new and interesting high energy features which may be useful for understanding the electronic properties of these materials. Using a perturbative approach, which allows the calculation of dynamical properties in the $t - J$ model, one-electron spectral properties were calculated. A strongly renormalized quasi-particle band near the Fermi surface and incoherent spectra at high energy were obtained. Among different current experimental interpretations, the obtained results are closer to the interpretation given by Pan *et al.*¹⁰. The self-energy shows large high energy contributions which are responsible for the incoherent structures showed by the spectral functions and the reduction of the quasiparticle weight and bandwidth. According to the calculation, collective charge fluctuations are the main source for the self-energy renormalizations. For testing if the obtained self-energy is compatible with transport measurement the resistivity versus temperature was estimated.

PACS numbers: 71.10.Fd, 71.27.+a, 79.60.-i

The understanding of high- T_c cuprates is one of the mayor challenges in solid state physics. Even with the problem unresolved, it is clear that not only the large value of the superconducting T_c is anomalous. Cuprates have also in common many electronic properties which are in clear contrast with the expected ones in usual metals. One of these, which is the subject of the present paper, is the one-electron renormalization obtained by angle-resolved photoemission spectroscopy (*ARPES*). Some years ago *ARPES* reported a kink in the electronic dispersion, at about $\sim 50 - 70 meV$, of hole doped cuprates^{1,2,3}. This kink indicates the presence of a small energy scale in the electronic self-energy. Besides the kink, early *ARPES* experiments¹ reported an imaginary part of the self-energy without sign of saturation up to energies of the order of $150 - 200 meV$. This feature, which was recovered in further experiments (see for instance Ref.[4]), indicates that besides low energy, high energy excitations are also present. However, since *ARPES* experiments were reported only for $\omega < 300 meV$ this discussion was postponed until very recently.

Recently, *ARPES* measurements^{5,6,7,8,9,10} reported results up to large energy $\omega \sim -1 eV$, clearly showing the presence of high energy self-energy renormalizations contributing to the spectral functions. The extracted $E - \mathbf{k}$ dispersion from momentum distribution curves seems to show a nearly vertical “dive”¹⁰ (also called “waterfall”⁷) at about $350 meV$. These experiments provide opportunity for new investigations about the electronic order behind cuprates. In spite of different experiments showing similar features, the interpretation is not unique^{5,6,7,8,9,10}. For instance, Xie *et al.*⁶ argue that, near the Fermi level, the quasiparticle band breaks at about $\sim -350 meV$ and, at higher energies follows the dispersion predicted by band structure calculation. Graf *et al.*⁷ interpreted their results in terms of the disintegration of low energy Zhang-Rice singlet and the re-

emergency of the band structure dispersion at high energies. Pan *et al.*¹⁰ state that, at low energy, there is a strongly renormalized coherent band, while the spectra is incoherent at high energies. In this picture the vertical “dive” can be seen as a coherent-incoherent crossover and therefore, high energy features are not related with band structure calculations.

In this paper, electronic spectral functions and self-energy corrections are investigated in the framework of the $t - J$ model. The obtained results are confronted with the experiments suggesting support for the scenario proposed by Pan *et al.*. The calculation of spectral properties in the $t - J$ model requires a controllable treatment of the non-double-occupancy constraint. While there are many calculations at mean field level, the evaluation of fluctuations above mean field, which is of interest for understanding dynamical properties as, for instance, the electronic self-energy, is very hard. Recently we have developed a large- N perturbative approach¹¹ (where the spin components have been generalized to N components) for the $t - J$ model based on the path integral representation for Hubbard operators. The advantage of this approach rests on the fact that it is formulated in terms of Hubbard operators as fundamental objects and, since there is no any decoupling scheme, problems that arise in other treatments are avoided, like considering fluctuations of the gauge field or Bose condensation that appears in the slave boson approach¹². It is not our aim to give here a detailed description of the method, it can be found in Refs.[11,13], only a brief summary is given in Fig.1. Using the Feynman diagrams (Fig.1a), the self-energy $\Sigma(\mathbf{k}, \omega)$ can be evaluated (Fig.1c) and with it, the spectral function $A(\mathbf{k}, \omega)$ can be obtained as usual. In Ref.[13], in order to test the confidence of our method, spectral functions were compared with those obtained using Lanczos diagonalization finding fairly good agreement. Also high energy self-energy

a) Propagators and vertices

$$G_{pp'}^{(0)} = \begin{array}{c} p \\ \longrightarrow \\ p' \end{array} \quad D_{ab}^{(0)} = \begin{array}{c} a \\ \dashrightarrow \\ b \end{array}$$

$$\Lambda_a^{pp'} = \begin{array}{c} p \\ \swarrow \quad \searrow \\ a \quad \quad \quad k, \omega_n \\ \swarrow \quad \searrow \\ q, v_n \quad \quad k', \omega'_n \\ p' \end{array} \quad \Lambda_{ab}^{pp'} = \begin{array}{c} a \quad \quad \quad p \\ \swarrow \quad \searrow \quad \swarrow \quad \searrow \\ q', v'_n \quad \quad k, \omega_n \\ \swarrow \quad \searrow \quad \swarrow \quad \searrow \\ q, v_n \quad \quad b \quad \quad k', \omega'_n \\ p' \end{array}$$

b) $\Pi_{ab} = \text{loop} + \text{loop}$
 $D_{ab}^{-1} = (\text{double dashed line})^{-1} = [D_{ab}^{(0)}]^{-1} - \Pi_{ab}$

c) $\Sigma = \Sigma^{(1)} + \Sigma^{(2)} = \text{loop} + \text{loop}$

FIG. 1: a) Solid line is the propagator, which is $O(1)$, for an electron with the dispersion E_k described in the text. Dashed line is the 6×6 boson propagator, which is $O(1/N)$, for the six component boson field δX^a . The component δX^1 corresponds to charge fluctuations, δX^2 is introduced to fulfil the non-double occupancy constraint, and δX^a , with a from 3 to 6, is associated with the Heisenberg coupling J . $\Lambda_a^{pp'}$ and $\Lambda_{ab}^{pp'}$ are the interaction vertices between two fermions and one and two bosons respectively. Vertices are $O(1)$ and were obtained from the effective theory constructed under the requirement that non-double occupancy and the Hubbard operators algebra be satisfied. Combining the order of vertices and propagators a given physical quantity can be evaluated at a given order of $1/N$. This counting means that the approach is controllable by the small parameter $1/N$. b) Irreducible boson self-energy Π_{ab} and the renormalized boson propagator (double dashed line). c) Contributions $\Sigma^{(1)}$ and $\Sigma^{(2)}$ to the electron self-energy $\Sigma(\mathbf{k}, \omega)$ through $O(1/N)$. In Σ , double dashed line, which contains collective charge fluctuations, can be seen as the excitations that interacting with fermions lead to the self-energy effects and incoherent structures discussed in the text.

excitations were identified but not compared with the new *ARPES* experiments^{5,6,7,8,9,10} which are more recent than Ref.[13].

Once presented the problem and the general characteristics of the method, results for the $tt' - J$ model are given. t and t' are the nearest and second-nearest neighbor hopping amplitudes respectively, and J is the Heisenberg coupling. In what follows we choose $t'/t = 0.35$, $J/t = 0.3^{14}$ and the calculation was done in the normal state. At mean field level the obtained electronic band is ($E_k = -2(t\delta/2 + \Delta)(\cos(k_x) + \cos(k_y)) + 4t'\delta/2\cos(k_x)\cos(k_y) - \mu$) where ($\Delta = J/2N_s \sum_k \cos(k_x)n_F(E_k)$) and μ the chemical potential. N_s is the number of sites and n_F the Fermi function. The bare (or mean field) band E_k (which already at this level is renormalized by correlations as shown by the presence of the doping δ and J) will be dynamically dressed by $\Sigma(\mathbf{k}, \omega)$. For these parameters, in the doping range of interest for cuprates, a hole-like Fermi surface is obtained. We also choose $\delta = 0.26$ which corresponds to highly overdoped regime

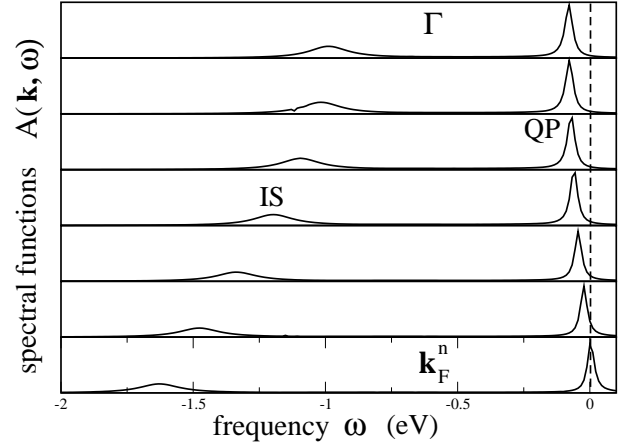


FIG. 2: Spectral functions along the nodal direction from Γ to the nodal Fermi vector \mathbf{k}_F^n . Close to the Fermi surface a strongly renormalized quasiparticle (QP) coherent band is obtained. For large energy ($\sim -1\text{eV}$) incoherent structure (IS) is observed. The vertical dashed line marks the Fermi level. All vertical scales are equal. When \mathbf{k} moves from Γ to \mathbf{k}_F^n , while the quasiparticle peak approaches $\omega = 0$, the incoherent structure moves in opposite direction in qualitative agreement with the experiment. See text for discussions.

where several *ARPES* experiments were performed^{6,10}. On the other hand, as discussed in Ref.[13], our method is better for large than for low doping. The existence of anomalous features in highly overdoped samples is very interesting because the system is far from the antiferromagnetic phase and the pseudogap, if it is not zero, is very weak. For $\delta = 0.26$ the nodal Fermi vector is $\mathbf{k}_F^n = (0.39, 0.39)\pi/a$.

Results for the spectral functions (energy distribution curves) along the nodal direction, from Γ ($0, 0$) to \mathbf{k}_F^n , are presented in Fig.2 where we adopt the accepted value $t = 0.4\text{eV}^{14}$. Close to the Fermi surface a highly renormalized parabolic quasiparticle coherent band is obtained. In addition, at high energy ($\sim -1\text{eV}$) incoherent structures are present. For the present parameters the quasiparticle weight results $Z = (1 - \frac{\partial \text{Re}\Sigma}{\partial \omega})^{-1} \sim 0.4$. The remainder spectral weight lies mainly in the incoherent structure. There is also spectral weight in the form of a tail between the quasiparticle and the incoherent structure and at $\omega > 0$ (Fig.4a).

Let us compare Fig.2 with the experiment^{6,10}. Similarly to Fig.1c in Xie *et al.*⁶, which is reproduced here in Fig.3a, Fig.2 shows that while the low energy peak moves toward the Fermi surface, the high energy structure disperses in opposite direction. A difference with the results in Xie *et al.* is the following. In their results the low energy peak is observed near \mathbf{k}_F^n , and away from it losses intensity being nearly invisible when approaching Γ (Fig.3a). This behavior is of fundamental interest

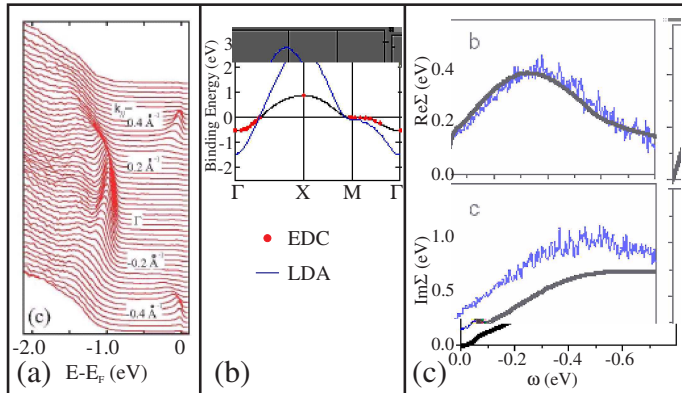


FIG. 3: (a) Fig.1c modified from Ref.[6] showing energy distribution curves (EDC) where low energy quasiparticle peaks and high energy features are observed. (b) Fig.4a modified from Ref.[10] where a strongly renormalized coherent band (full circles) is reported near Γ . Notice the bandwidth reduction with respect to the band structure calculation (LDA). (c) Figs.4b and 4c modified from Ref.[5] showing the real and imaginary parts of the self-energy.

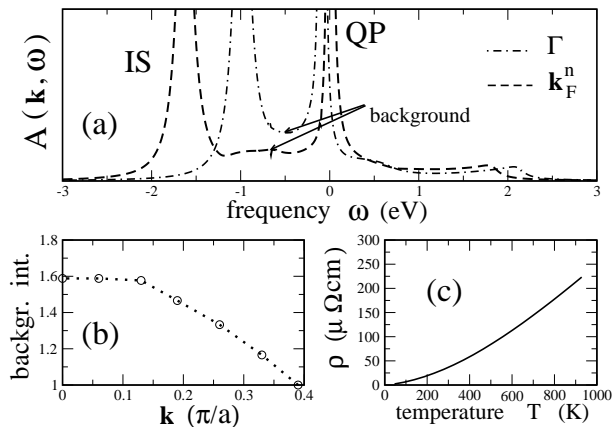


FIG. 4: (a) Spectral functions for the Γ and k_F^n vectors using an appropriate vertical scale in order to see the spectral weight in the background between the quasiparticle (QP) and the incoherent structure (IS). The spectral weight for $\omega > 0$ is also shown. (b) Background intensity (normalized to the background intensity at k_F^n) vs k from Γ to k_F^n . (a) and (b) show that the intensity of the background increases when approaching Γ . (c) Resistivity ρ vs temperature T . ρ was estimated using the procedure described in the text. The resistivity values are in the order of magnitude of the experiments^{25,26}. In addition, ρ vs T presents a fractional power law $\rho \sim T^m$ where $m \sim 1.6 - 1.7$. $\omega_p = 2\text{eV}$ was chosen (see text).

for the “waterfall” interpretation. The vanishing of the quasiparticle intensity near Γ suggests that the low energy dispersion evolves abruptly to the high energy features. It is important to notice that our Fig.2 does not exhibit the mentioned intensity decreasing away from the Fermi surface and shows well defined quasiparticles and incoherent structures for all \mathbf{k} -vectors. It is not clear which is the reason for the experimental decreasing of the low energy peak intensity. Notice that the predicted quasiparticle weight Z is small, thus probably hard to follow experimentally away from the Fermi surface because it may become mixed with the background as discussed below. In spite of the intensity decreasing away from k_F^n , Pan *et al.*¹⁰ resolved the quasiparticle peak approaching Γ (see Fig.1e and Fig.4a in Ref.[10], Fig.4a is reproduced here in Fig.3b) following a parabolic shape and, at the same time, high energy spectral features are observed (see Fig.1d in that paper) as in our Fig.2. Our calculated quasiparticle bandwidth is somewhat smaller than in the experiment. We think that the existence of low energy quasiparticle peaks near Γ make doubtful the interpretation in terms of only one feature evolving from low to high energies. Using Lanczos diagonalization on the $t - J$ model, similar high energy spectral features were reported in Ref.[15] (see also Ref.[16]).

In Ref.[10] it was observed that the “diving” behavior, which is mainly inferred from momentum distribution curves, is not manifested in the energy distribution curves, instead, an enhancement of the background of the energy distribution curves is observed near Γ (see Fig.1f in Pan *et al.*) making difficult the quasiparticle peak detection. Thus, the background enhancement may be important for understanding differences between momentum and energy distribution curves. In Fig.4a we present spectral function results at Γ and k_F^n using an appropriate vertical scale in order to see the spectral weight in the background between the quasiparticle and the incoherent structure. In Fig.4b the background intensity, normalized to the background intensity at k_F^n , is plotted as a function of \mathbf{k} from Γ to k_F^n . Clearly, the background increases from k_F^n to Γ . Other unknown effects¹⁷, contributing to the background, are probably present because the predicted quasiparticle intensity near Γ seems to be larger than in the experiment however, the calculation shows, qualitatively, common features with the experiment. The preceding discussion and the existence of the quasiparticle near Γ put our results closer to the interpretation given by Pan *et al.*; near the Fermi surface a strongly renormalized parabolic coherent band is present and the vertical “dive” is likely the incoherent part.

In recent *ARPES* experiments⁹ high energy features were discussed as a function of doping showing that their energy position decreases with increasing doping (see Fig.1 in that paper). This behavior is consistent with the expected one in our calculation (see Figs.3-5 in Ref.[13]). On the other hand, in Ref.[9], it was also obtained that high energy features lie at higher energies than the pre-

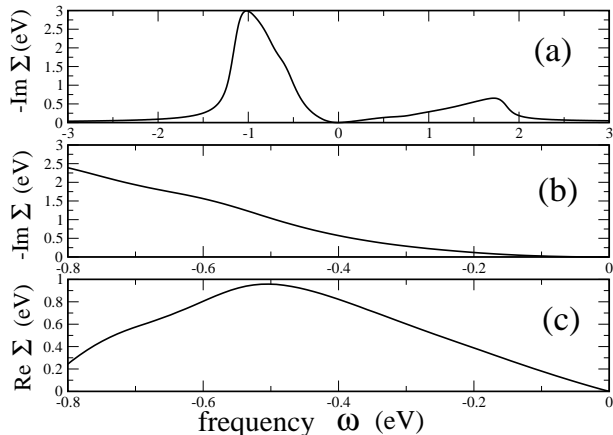


FIG. 5: (a) $-Im\Sigma(k_F^n, \omega)$ vs ω in the full range of frequency. The self-energy is strongly asymmetric around $\omega = 0$ reflecting differences between the addition and removal of a single electron in a correlated system. $Im\Sigma$ shows large structures at large energies and no sign of saturation up to energies of $\sim -1eV$ is observed. These large structures are the responsible for the incoherent features described in Fig.2 and are mainly due to collective charge fluctuations (see text for discussions). Since high energy features are due to collective charge fluctuations they are very robust against the value of J . (b) and (c) are $-Im\Sigma(k_F^n, \omega)$, and $Re\Sigma(k_F^n, \omega)$ vs ω respectively, for $-0.8eV < \omega < 0$.

dictions of the band structure calculations. This behavior, which is anomalous because interactions should reduce the bandwidth, to our opinion, may be considered as an additional support for the interpretation of the high energy features in terms of incoherent structures due to electronic correlations.

Self energy results are presented in Fig.5 for $\mathbf{k} = \mathbf{k}_F^n$. In panel (a), $-Im\Sigma(k_F^n, \omega)$, in the full range of frequency, is shown. $\Sigma(\mathbf{k}, \omega)$ is strongly asymmetric with respect to $\omega = 0$ which is due to the difference between the addition and removal of a single electron in a correlated system. Notice that the self-energy presents large structure at large energy with no sign of saturation up to energies of $\sim -1eV$. For a better comparison with the self-energy behavior reported by the recent *ARPES* measurements, the imaginary and real parts of the self energy are presented in panels (b) and (c), respectively, for the energy range $-0.8eV < \omega < 0$. Interestingly, both $Re\Sigma$ and $Im\Sigma$ present similar shape and order of magnitude to the experiment^{5,6}. For instance, $Re\Sigma$ (Fig.5c) shows a maximum of the order of $\sim 0.9eV$ at about $\sim -0.5eV$. (In Fig.3c, Figs.4b and 4c from Ref.[5] are reproduced for comparison with Fig.5). This behavior, as discussed in Ref.[5], is in contrast with previous reports where the self-energy spread out over a much lower energy scale⁴. Therefore, our self-energy shows a large energy scale of the order of $1eV$ which is responsible for the incoherent

structure showed by the spectral functions.

Finally, at low energies, the $Re\Sigma$ (Fig.5c) presents only one slope while in the experiments^{5,6} two slopes can be seen; above and below $\sim 50meV$ (Fig.3c). Since the lower slope is larger than the upper one^{5,6}, we may associate the upper slope as originated by electronic high energy contributions while, at low energy there are additional contributions, associated with the former kink^{1,2,3}. According to Ref.[5] the spectral weight of these low energy excitations is only $\sim 10\%$ of the full spectra. From Fig.5c, our estimated slope is $\lambda = -\frac{\partial Re\Sigma}{\partial \omega} \sim 1.5$ which is close to the experimental upper slope seen for $\omega > 50meV$. We take this fact as an additional support for considering that high energy features are contained in our description. Even when in this paper we are mainly interested on the high energy features a few statements about the low energy kink are noteworthy. Our self-energy (Fig.5) does not show any low energy scale however, this is not crucial because, after much discussion, the origin of the kink remains open⁴ and one possibility is that the kink is due to phonons^{18,19}. If this is the case, a pure $tt' - J$ model calculation, as in present case, does not account for the expected low energy self-energy renormalizations. From the pure $t - J$ model low energy spectral features of magnetic origin may also be expected¹⁵ however, they should be weaker for highly overdoped than for underdoped samples which is not clear from the experiments. According to results in Ref.[15] the spectral weight of low energy spectral features is a fraction of the quasiparticle weight and then, presumably small.

Let us discuss the origin of the high energy features. In Ref.[5], they are associated with magnetic excitations. However, since these features are present in highly overdoped samples where magnetism is very weak, we take this interpretation with caution. Our model calculation suggests that they are due to charge fluctuations. In the usual many body language, self-energy can be expressed in terms of $\alpha^2 F(\omega)$, where the notation is such that $F(\omega)$ gives information of the density of state of a boson interacting with electrons, and α^2 about the coupling. In Ref.[13] it was shown that collective charge fluctuations, playing the role of bosonic excitations, are the main contribution to $\alpha^2 F(\omega)$ and they lead to strong incoherent features at high energies. Collective charge fluctuations discussed here are similar to those reported by inelastic x-rays scattering^{20,21}. Two recent theoretical papers^{22,23} have considered spin fluctuations for explaining the high energy features. In both calculations, self-energy renormalizations suggest an abrupt evolution (high energy kink) of the low energy quasiparticle peak to the high energy features. This scenario is different to the ours, where a low energy coherent quasiparticle band coexists with high energy incoherent structures. In addition, based on RPA calculations, charge fluctuations were ruled out in Ref.[23]. In contrast, in our approach, collective charge fluctuations, when they are treated in the strong coupling limit of the $t - J$ model, lead to a self-energy (more stronger and asymmetric than RPA)

which produces the results discussed in present paper.

It is important to test, to what extent, $\Sigma(\mathbf{k}, \omega)$ from *ARPES* is compatible with transport measurements. In order to get some insight into this problem, the resistivity ρ vs temperature T is shown in Fig.4c. For estimating the resistivity it was used the expression $\rho(T) = \frac{4\pi}{\omega_p^2} \frac{1}{\tau}(T)$, where $\frac{1}{\tau}(T) = -2Im\Sigma(\omega = 0, T)$. It is known that $1/\tau$ is related with the $Im(\Sigma)$ averaged over the Fermi surface using the weight factor $(1 - \cos\theta)$, however our self-energy is very isotropic over the Fermi surface and then, $1/\tau$ is very close to $-2Im(\Sigma)$. For the plasma frequency we choose $\omega_p = 2eV^{24,25}$. In spite of the approximations and the fact that impurities may also contribute, the resistivity values are in the order of magnitude of the experiments^{25,26}. Interestingly, we found a fractional power law behavior $\rho \sim T^m$ with $m = 1.6 - 1.7$

which is close to that reported in Refs.[25,27] for overdoped regime. This fractional power law was discussed in Ref.[28] as indication of an anomalous Fermi liquid behavior in overdoped cuprates.

In conclusion, we have studied high energy *ARPES* spectral features in the framework of the $tt' - J$ model. Results for spectral functions $A(\mathbf{k}, \omega)$ and self-energy $\Sigma(\mathbf{k}, \omega)$ were presented and confronted with the experiments. A strongly renormalized quasiparticle parabolic band was obtained near the Fermi surface and incoherent structures exist at large energy ($\sim -1eV$). The present results support the experimental interpretation given by Pan *et al.*¹⁰.

The author thanks to M. Bejas and A. Foussats for valuable discussion and H. Parent for critical reading the manuscript.

-
- ¹ T. Valla *et al.*, *Science* 285 (1999) 2110.
² P. V. Bogdanov *et al.*, *Phys. Rev. Lett.* 85 (2000) 2581.
³ A. Kaminski *et al.*, *Phys. Rev. Lett.* 86 (2001) 1070.
⁴ A. A. Kordyuk *et al.*, *Phys. Rev. Lett.* 97 (2006) 017002.
⁵ T. Valla *et al.*, *cond-mat/0610249*.
⁶ B. Xie *et al.*, *cond-mat/0607450*.
⁷ J. Graf *et al.*, *Phys. Rev. Lett.* 98 (2007) 067004.
⁸ J. Chang *et al.*, *cond-mat/0610880*.
⁹ W. Meevasana *et al.*, *cond-mat/0612541*.
¹⁰ Z.-H. Pan *et al.*, *cond-mat/0610442*.
¹¹ A. Foussats, A. Greco, *Phys. Rev. B* 70 (2004) 205123.
¹² P. A. Lee, N. Nagaosa, X.-G. Wen, *Rev. Mod. Phys.* 78 (2006) 17.
¹³ M. Bejas, A. Greco, A. Foussats, *Phys. Rev. B* 73 (2006) 245104.
¹⁴ E. Dagotto, *Rev. Mod. Phys.* 66 (1994) 763.
¹⁵ A. Moreo, S. Haas, A. W. Sandvik, E. Dagotto, *Phys. Rev. B* 51 (1995) 12045.
¹⁶ W. Stephan, P. Horsch, *Phys. Rev. Lett.* 66 (1991) 2258.
¹⁷ Recently (Kordyuk *et al.*, *cond-mat/0702374* and Alexandrov and Reynolds, *cond-mat/0702609*) it has been pointed out that the experiments can be influenced by *ARPES* matrix element effects, which may cause a suppression of the photoemission intensity in some directions of the Brillouin zone. It is important to notice that the discussion about the influence of these effects is open (see Ref.[7]). As stressed in the paper, our calculation suggests that the low energy renormalized coherent band and high energy incoherent structures are strong enough to be observed. For instance, the predicted high energy incoherent features carry $\sim 40\%$ of the spectral weight (what is close to the quasiparticle weight Z) and they occur at a well defined energy value thus, in principle, hard to mask.
¹⁸ Z. Shen, A. Lanzara, N. Nagaosa, *cond-mat/0102244*.
¹⁹ R. Zeyher, A. Greco, *Phys. Rev. B* 64 (2001) R140510. A. Greco, A. Dorby, *Solid State Communications* 122 (2001) 111.
²⁰ M. Z. Hasan, *et al.*, *Science* 288 (2000) 1811.
²¹ R. Markiewicz, A. Bansil, *Phys. Rev. Lett.* 96 (2006) 107005.
²² A. Macridin *et al.*, *cond-mat/0701429*.
²³ R. S. Markiewicz, S. Sahrakorpi and A. Bansil, *cond-mat/0701524*.
²⁴ J. Hwang, T. Timusk, G. Gu, *cond-mat/0607653*.
²⁵ Y. Ma, N. Wang, *Phys. Rev. B* 73 (2006) 144503.
²⁶ T. Timusk, B. Statt, *Rep. Prog. Phys.* 62 (1999) 61.
²⁷ K. Yang *et al.*, *cond-mat/0602418*.
²⁸ H. Castro, G. Deutscher, *Phys. Rev. B* 70 (2004) 174511.